Analysis of predictor equations for determining the blast-induced vibration in rock blasting

International Journal of Mining Science and Technology 29 (2019) 905–915

Contents lists available at ScienceDirect

International Journal of Mining Science and Technology

journal homepage: www.elsevier.com/locate/ijmst

Analysis of predictor equations for determining the blast-induced vibration in rock blasting

Marilena Cardu [a,b,*], Dario Coragliotto [c], Pierpaolo Oreste [a,b]

[a] DIATI Politecnico di Torino, 10129 Torino, Italy
[b] IGG-CNR, Torino 10129, Italy
[c] Lochaline Quartz Sand Ltd., Lochaline Mine, PA80 5LQ Morvern, Scotland, United Kingdom

ARTICLE INFO

Article history:
Received 12 June 2018
Received in revised form 2 October 2018
Accepted 28 February 2019
Available online 7 March 2019

Keywords:
Rock blasting
Vibrations
Predictor equation
Site law
K-statistics
K-exponential

ABSTRACT

The paper proposes a new empirical correlation designed to complement the "site laws" currently used to evaluate the attenuation in the rock masses of vibrations induced by rock blasting. The formula contains a deformed exponential known as the K-exponential, which seems to well represent a large number of both natural and artificial phenomena ranging from astrophysics to quantum mechanics, with some extension in the field of economics and finance. Experimental validation of the formula was performed via the analysis of vibration data covering a number of case studies, which differed in terms of both operation and rock type. A total of 12 experimental cases were analysed and the proposed formulation exhibited a good performance in 11 of them. In particular, the proposed law, which was built using blast test data, produced very good approximations of the points representing the vibration measurements and would thus be useful in organising production blasts. However, the developed formula was found to work less well when a correlation obtained for a given site was applied to another presenting similar types of rocks and operations, and thus should not be employed in the absence of measurements from test data.

1. Introduction

A "site law" (predictor equation) can be defined as the mathematical expression to describe the attenuation of the vibrations in the rock masses produced by blasting; the site law is not characteristic of a site but rather, at most, of a particular kind of process, performed within a range of operating conditions, at a given site. The term "site law" is rather common referring to a predictor equation, obtained from experimental data concerning the monitoring of vibrations in a specific site, and effective only in relation to that site [1–4]. The formulas used as predictors are numerous, but can essentially be grouped into two categories: those that are based on the concept of scaled distance and those that are not. The former contain only two variables and can be simply determined by statistically processing the measured data; for this reason they are widely used, even though the latter are perhaps more satisfactory from a conceptual point of view.

Over the past 60 years, many researchers have studied the phenomenon of vibrations induced by explosives, with empirical laws formulated based on experimental blast tests or even production blasts [5–14]. Most of these studies have suggested that the parameter that best correlates with both the energy developed from the explosion and the stress suffered by the rock-mass and nearby structures is the vibration velocity or, more precisely, the peak particle velocity *ppv*, expressed according to the following equation:

$$ppv = k \cdot R^a \cdot Q^b \tag{1}$$

where *ppv* is the peak particle velocity, mm/s; R the distance between the barycenter of the charge and the point of vibration detection, m; Q the charge per delay, kg; and k, a and b the experimental constants depending on the blast geometry and rock type, generally, $0.5 \le a \le 1$ and $-1.5 \le b \le -1$.

In the case of blast tests, a chart is commonly used that correlates *ppv* with scaled distance, with the latter generally represented by the ratio between the distance R and the square or cubic root of the charge per delay Q; typically, the square root is used when the blast-survey point distance is greater than 30 m:

$$ppv = k \cdot \left(\frac{R}{\sqrt{Q}}\right)^{-m} \tag{2}$$

In contrast, for short distances, it is customary to use the cubic root of the charge for delay:

* Corresponding author at: DIATI Politecnico di Torino, 10129 Torino, Italy.
E-mail address: marilena.cardu@polito.it (M. Cardu).

https://doi.org/10.1016/j.ijmst.2019.02.009
2095-2686/

$$ppv = k \cdot \left(\frac{R}{\sqrt[3]{Q}}\right)^{-m} \tag{3}$$

where k and m are experimental coefficients; and m is always greater than 0.

The classic Eq. (2) would appear, on average, less unreliable than others; the unreliability of extrapolation over long distances, however, is of little weight in some cases (i.e. tunnel excavation, where relatively small charges per delay are used, that at distances of around 100 m give a disturbance almost always tolerable). More serious is the defect, common to all site laws, to provide uncertain predictions about what happens at very small distances, just beyond 3–4 times the diameter of the holes: in this case, it is assumed that the charge is point-like and that the distance from the point where the disturbance is detected is the distance from the centre of gravity of the charge, where it can be assumed that the whole explosive is concentrated.

The results obtained must, anyhow, be compared with the limits of the reference regulations; in Italy the German DIN4150 standard is commonly employed, which is more cautious than others in use in Europe.

Over the years, several different laws have been developed that differ not only in their prediction of the *ppv* values for large distances, but also from case to case, or from site to site [5,14–26].

Aimed at improving the current situation, an attempt was made to assess whether the proposal for a new empirical correlation could provide greater reliability in representing the attenuation of the intensity of vibrations caused by blasting in a rock mass, at different distances and charges per delay. This innovative correlation is based on the deformed exponential known as the K-exponential, recently used in numerous fields of physics.

2. K-exponential distribution

The so-called principle of kinetic interaction imposes the generalised form of entropy associated with a system and allows the acquisition of the statistical particle distribution as a stationary solution to nonlinear equations of evolution (a state which maximizes the generalised entropy) [27]. In recent decades, intense discussions have taken place regarding the use of classical or quantum unconventional statistics, with different forms of entropy considered for each [28–40]. A new statistical distribution, the K-deformed distribution, has been proposed both as a stationary solution to a nonlinear evolution equation and using the principle of maximum entropy [41–44]. The main mathematical properties of the deformed exponential function are summarised by the exponential $expK(x)$, where K is the deformation parameter; it has been postulated that this exponential obeys the following relationship:

$$expK(x) * expK(-x) = 1 \tag{4}$$

Each function $A(x)$ can be written as: $A(x) = Ae(x) + Ao(x)$, where $Ae(x) = Ae(-x)$ is an even function and $Ao(x) = -Ao(-x)$ is an odd function. The condition $A(x) * A(-x) = 1$ enables the expression of $Ae(x)$ as $Ao(x)$ through $Ae(x) = \sqrt{1 + A_{0(x)^2}}$; then, the function $A(x)$ can be written as $A(x) = \sqrt{1 + A_{0(x)^2}} + A_{o(x)}$

A number of the particularities of such K-statistics were here adopted in order to obtain a distribution function with which to study the vibrations induced by explosives as a function of the charge per delay (*cpd*) Q and distance R. In statis tical physics, a typical distribution function can be written in the form:

$$f_i = A\chi(x) \tag{5}$$

where the $\chi(x)$ function, for $x \to 0$, is:

$$\chi(x) \to exp(-x) \tag{6}$$

It has been observed that the function $\chi(x)$, for high x values, deviates from the ordinary exponential function and can be better described by a power function:

$$\chi(x) \sim x^{-1/K} for\, x \to \infty \tag{7}$$

This type of distribution has been observed in an extremely wide range of scientific applications, including, for instance: cosmic rays, processes of particles production, fluid dynamics, turbulence, seismology, meteorology, biology; applied finance, socio-demographics, language and even fields that involve more generally human activities [45–64]. Here the theory developed by Kaniadaki is employed to estimate the function $\chi(x)$ in the form [26,65–67].

$$\chi(x) = expK(-x) \tag{8}$$

$$\text{with } expK(x) = \left[\sqrt{1 + K^2x^2} + Kx\right]^{1/K} \tag{9}$$

The latter function represents the deformation to a parameter $(0 < K < 1)$ of the ordinary exponential retrieved for the limit $K \to 0$, whereas the associated distribution function:

$$f_i = AexpK(-bx) \tag{10}$$

Approximates the ordinary exponential is for low values of x; it presents a queue with a trend similar to a power law for high x values. The experimental data from both blast tests and production blasts can thus be analysed using Eq. (10), where f_i is the *ppv* and x is the scaled distance *SD* [68–70].

$$ppv = AexpK(-bSD) \tag{11}$$

that is:

$$ppv = AexpK\left(-b\frac{R}{Q^d}\right) \tag{12}$$

corresponding to:

$$ppv = A\left[\sqrt{1 + K^2\left(-b\frac{R}{Q^d}\right)^2} + K\left(-b\frac{R}{Q^d}\right)\right]^{1/K} \tag{13}$$

There are thus four parameters or "site constants" to be considered: A, b, K, and d.

3. Analysis of vibration data using the new formula

The four site parameters established in Eq. (12) and the relative error were calculated for 12 case studies. Parameter values were obtained by identifying the four constants A, b, K and d that minimise the error of the empirical correlation compared to the experimental data; in other words, the values of the parameters that minimise the sum of the squared deviations amongst experimental values and those approximated by the curve representing the empirical correlation, or "*expK*", were calculated. Mathematical techniques, aimed at finding the minimum error condition, have been used in order to finally identify, accurately and quickly, the set of the best parameters.

In the latter case study, a devoted measurement campaign was carried out in order to verify whether the curve built on the basis of the preliminary blast tests could reliably approximate the points referred to by the pairs of values (*PPV*, *SD*) measured during the production blasting.

In every experimental case, both the error, calculated as the sum of the squared deviations between the value of *ppv* approximated by the curve and the measured value, and the standard deviation with respect to the obtained curve, were evaluated. The analysed cases, all of them referring to civil or mining operations

for the most part located in Northern Italy, are described in the following, and the results obtained are highlighted.

3.1. Case 1: excavation of a trench to build a highway

The example refers to blast tests where the drill and blast technique was used to build a highway. Vibration monitoring was required due to the presence of a settlement at a short distance (Fig. 1).

The curve, corresponding to the Eq. (12) that best approximates the experimental points, is given in Fig. 2.

As noted in Fig. 2, the values of the parameters referred to Eq. (12) are: A is 6755292, b 534,27, K 0,7096, and d 0,4465.

3.2. Case 2: marlstone quarry

Experimental blast tests were carried out in a marlstone quarry located in Northern Italy. The target of the research was to monitor ground vibrations through the *ppv* control, to protect the dwelling area close to the quarry, as quoted in study by Giraudi [71]. The distance from blasting sites to surrounding buildings was between 70 and 200 m. To define a suitable charge per delay during the exploitation, two experimental blasts were performed, with the same geometry: burden 2.5 m; spacing 2.5 m; stemming between 1.7 and 2.6 m; hole diameter 64 mm. Three blast-holes per blast were initiated. For each blast, the boreholes were charged with 1.5, 2.5, and 3.5 kg of emulsion explosives, respectively. The initiation system was setup by three non-electric detonators with 0, 300 and 600 ms delay at the bottom of the boreholes. An electric detonator was used as source of initiating pulse. Both soil material and drilling cuttings were combined, and used as stemming. In Figs. 3 and 4, the geometry of the two experimental blasts is depicted.

The *ppv* data were obtained through the analysis of the measurements recorded by six tri-axial geophones, that were positioned at different distances from the blasting site. Figs. 5–8 show, as an example, the vibration records related to the two experimental blasts recorded by two of the six tri-axial geophones used in the campaign. The curve, corresponding to Eq. (12), that best approximates the experimental points, is given in Fig. 9.

As noted in Fig. 9, the values of the parameters referred to Eq. (12) are: A is 39140, b 120,006, K 0,7899, and d 2,1074.

3.3. Case 3: limestone quarry

The case refers to an experimental campaign that was made in a limestone quarry in Northern Italy. The excavation geometry of the production blasts is: burden 2.5 m, spacing 3 m, stemming 2 m, drilling diameter 76 mm. The total charge (emulsion explosive) varied from 90 to 214 kg (6 to 14 blast-holes); the nonel initiation system was employed, with 25 ms delays; the powder factor did not exceed 0.14 kg/m^3. The *ppv* data were obtained through the analysis of the measurements recorded by nine tri-axial geophones, that were positioned at different distances from the blasting site. The curve, corresponding to Eq. (12), that best approximates the experimental points, is given in Fig. 10.

As noted in Fig. 10, the values of the parameters referred to Eq. (12) are: A is 128,71, b 1,8955, $K \sim 0$, and d 1,444.

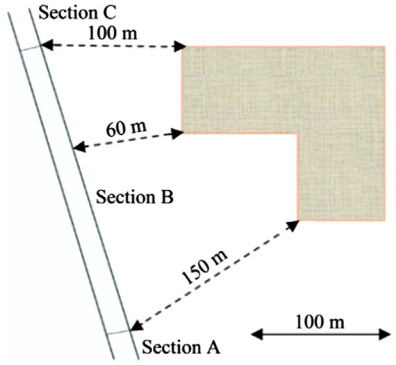

Fig. 1. Route of the motorway and schematic representation of the distances from the settlement.

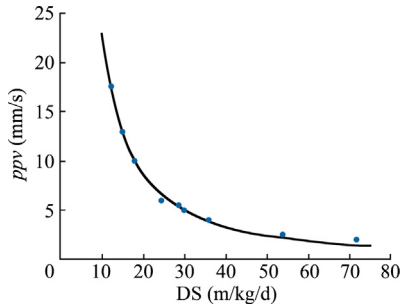

Fig. 2. Representation of the experimental points and best fit curve obtained through the k exponential formulation for case 1.

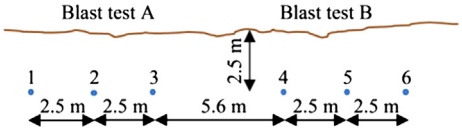

Fig. 3. Plan view of the drilling pattern adopted during the experimental blasts.

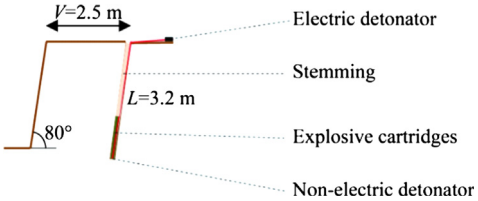

Fig. 4. Cross section of a blasthole.

3.4. Case 4: limestone quarry

The case refers to the data coming from an experimental campaign that was made in a limestone quarry in Central Italy. The monitoring had the aim of establishing the max charge per delay in the production blasts, to avoid damages to the residential buildings close to the quarry.

The geometry of the blasting pattern was: burden 2.5 m, spacing 2.5 m, stemming 2.5 m and drilling diameter 89 mm. Each hole was loaded with 10 kg of emulsion. An example of blast is given in Fig. 11.

The triggering system was composed of 6 electric detonators, one of which instantaneous, 2 with 225 ms delay and 3 with 450 ms delay, corresponding to the numbers 0, 9, 18 of the 25 ms series, positioned at the top of each blast-hole. A strand of 15 g/m detonating cord was also provided for each blast-hole.

The curve, corresponding to Eq. (12), that best approximates the experimental points, is given in Fig. 12.

As noted in Fig. 12, the values of the parameters referred to Eq. (12) are: A is 363963, b 4641,01, K 0,8939, and d 1,008.

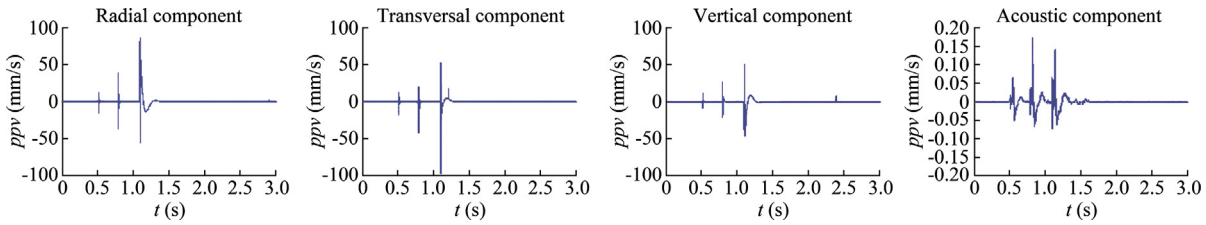

Fig. 5. Blast test A–acoustic recording and trend of the three seismic components recorded by geophone 1, placed at a distance of about 14 m from the blast.

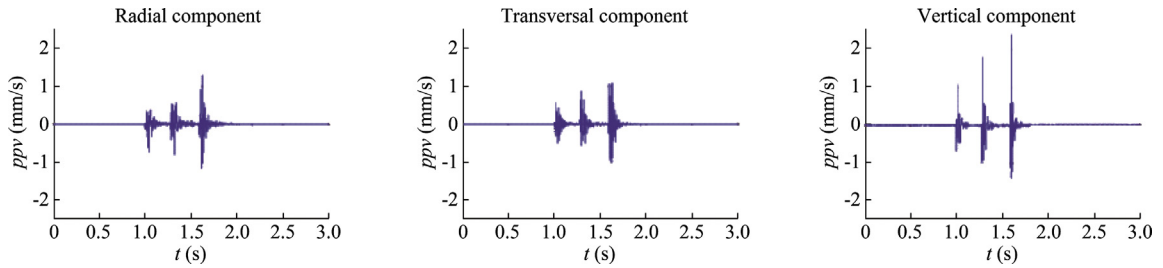

Fig. 6. Blast test A–trend of the three seismic components recorded by geophone 4, placed at a distance of about 97 m from the blast.

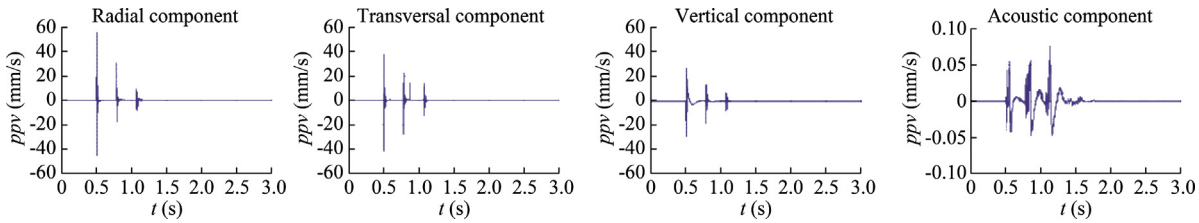

Fig. 7. Blast test B–acoustic recording and trend of the three seismic components recorded by geophone 1, placed at a distance of about 17 m from the blast.

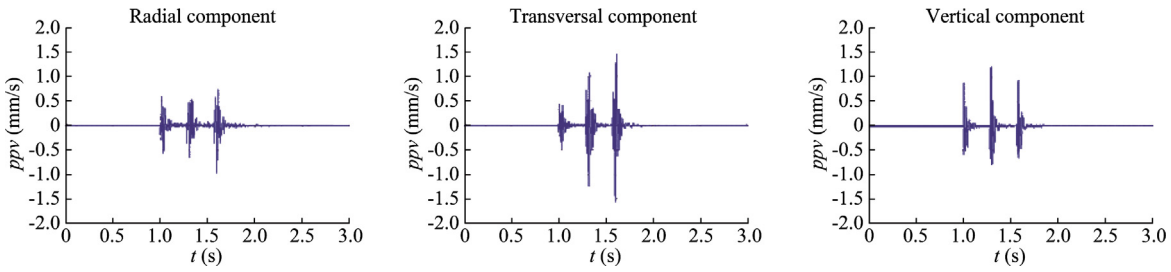

Fig. 8. Blast test B–Trend of the three seismic components recorded by geophone 4, placed at a distance of about 98 m from the blast.

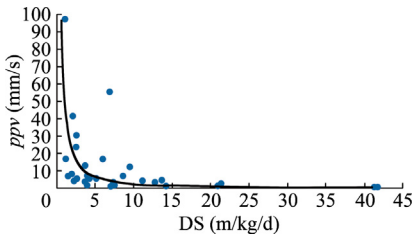

Fig. 9. Representation of the experimental points and best fit curve obtained through the k exponential formulation for case 2.

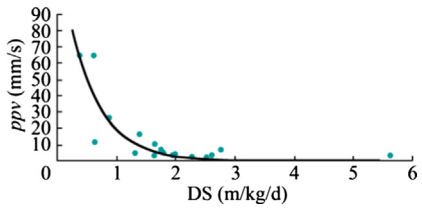

Fig. 10. Representation of the experimental points and best fit curve obtained through the k exponential formulation for case 3.

3.5. Case 5: excavation of a shaft-tunnel system in limestone

The experimental campaign was realized to identify the max charge per delay to use during a civil excavation (limestone rock). The limitation of the vibration was necessary for two reasons: the stability of the rock face and the need to preserve the integrity of a historic building, a sanctuary built on the side of Maggiore Lake, Italy. The aim of the excavation was to create a shaft for an elevator and a tunnel to facilitate the access to this remote site of historic, artistic and religious importance. A scheme of the project is given in Fig. 13. Measurements were carried out in different parts of the

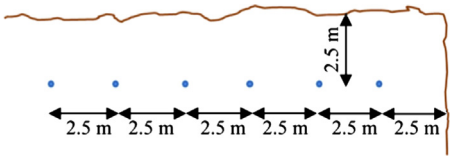

Fig. 11. Plan view of an experimental blast.

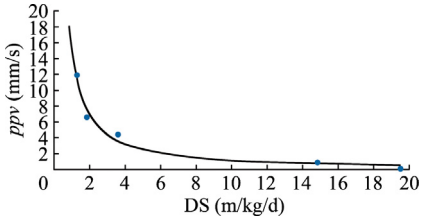

Fig. 12. Representation of the experimental points and best fit curve obtained through the k exponential formulation for case 4.

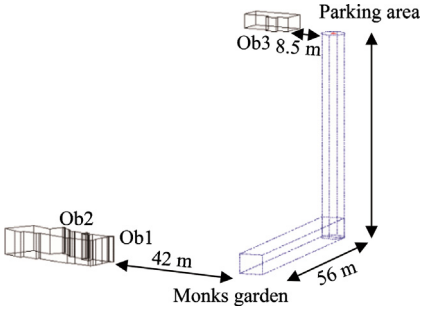

Fig. 13. Shaft equipped with a lifting system, connecting the top hill level (254 m above sea level), to the down hill level (203 m above sea level); section shaft: 28 m^2.

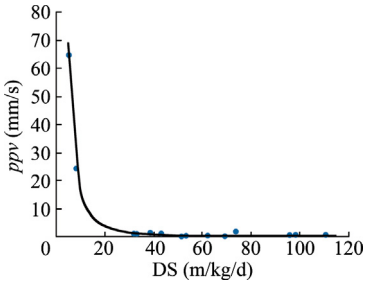

Fig. 14. Approximation of the experimental data for case 5, using the k exponential formulation.

complex and in the upper part of the wall in the vicinity of other buildings, as reported by [72]. The charge per delay limit found was in the 0.5–1 kg range for a great part of the excavation work and, consequently, the pull of the rounds very seldom could exceed 1 m (at the cost of a very high specific drilling).

As shown in Fig. 13, horizontal tunnel is connecting the gardens to the bottom of the shaft, and section tunnel is 25 m^2.

The area where the blast tests took place is the same where both the shaft and the access tunnel would have built.

The curve, corresponding to Eq. (12), that best approximates the experimental points, is given in Fig. 14.

As noted in Fig. 14, the values of the parameters referred to Eq. (12) are: A is 2149576; b 30,57, K 0,4826, and d 0,6955.

3.6. Case 6: underground gypsum quarry

The monitoring campaign was made in an underground quarry in North Italy, exploited by rooms and pillars. In proximity of the quarry there are many towns that must be preserved by the vibrations induced by blasting. Several production blasts were monitored; the max charges per delay ranged from 10 to 14,55 kg, while the measuring points were at varying distances from the source (20 m to almost 500 m). A drilling diameter of 51 mm was used, with a theoretical pull of 3.1 m; the holes were loaded with gelatin dynamite and emulsion cartridges (38–40 mm diameter). In Fig. 15 a picture of the quarry site is given. Fig. 16 shows a typical blast performed at the quarry.

The curve, corresponding to Eq. (12), that best approximates the experimental points, is given in Fig. 17.

As noted in Fig. 17, the values of the parameters referred to Eq. (12) are: A is 110101; b 9,0828; K 0,7017, and $d \sim 0$.

3.7. Case 7: limestone quarry

The experimental campaign refers to a limestone quarry located in North Italy. The monitoring was performed to obtain a site law aimed to evaluate the maximum charge per delay employable in view of the expansion of the site. The production blasts were monitored during a 6-months period. Blasts were organized with a cpd of 7.24 kg. A scheme of a typical blast is given in Fig. 18.

As noted in Fig. 18, the numbers refer to the blasting sequence. The blast-holes of the same row are connected with 25 ms nonel units; between a row and the next 17 ms units are employed, so as to avoid the superposition of the effects, ensuring that there is always at least a 8 ms delay between the blast-holes, and 500 ms delay at the bottom.

The curve, corresponding to Eq. (12), that best approximates the experimental points, is given in Fig. 19.

As noted in Fig. 19, the values of the parameters referred to Eq. (12) are: A is 78959, b 9,64, K 0,73, and d 0.

3.8. Case 8: marlstone mine

The case presents the results of the experimental measurements performed in a marlstone open-pit mine in the province of Varese, North Italy. A general view of the site is given in Fig. 20.

The curve, corresponding to Eq. (12), that best approximates the experimental points, is given in Fig. 21.

As noted in Fig. 21, the values of the parameters referred to Eq. (12) are: A is 182603, b 4,48, K 0,4078, d 0,5577.

3.9. Case 9: limestone quarry

The case presents the results of the experimental measurements performed during a campaign in a limestone open-pit quarry in the province of Como, Northern Italy.

The curve, corresponding to Eq. (12), that best approximates the experimental points, is given in Fig. 22.

Fig. 15. Quarry site analyzed and the room-pillars system is clearly noticeable.

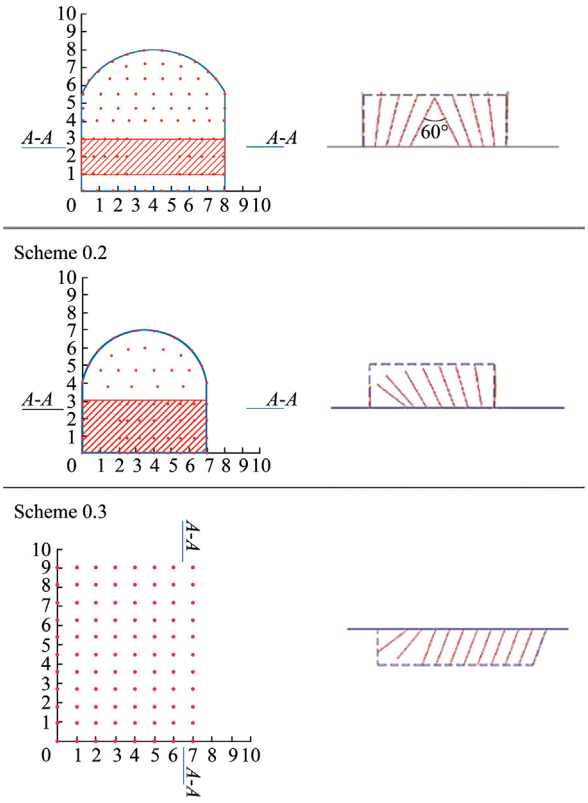

Fig. 16. Schemes of the blasts adopted at the quarry [73].

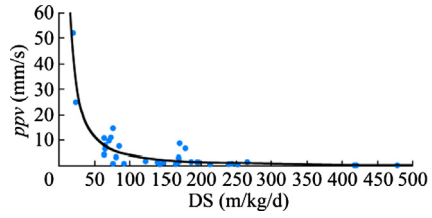

Fig. 17. Approximation of the experimental data for case 6, using the *k* exponential formulation.

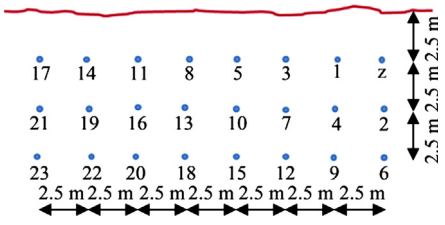

Fig. 18. Plan view of a production blast.

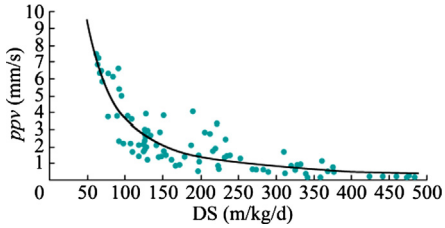

Fig. 19. Approximation of the experimental data for case 7, using the *k* exponential formulation.

Fig. 20. A general view of the quarry site after a production blast on a bench.

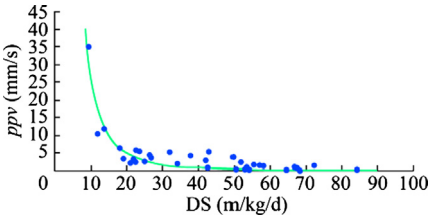

Fig. 21. Approximation of the experimental data for case 8, using the k exponential formulation.

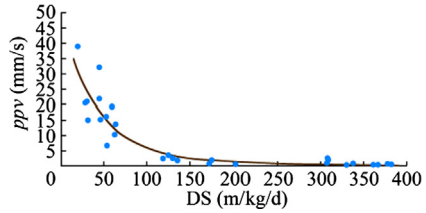

Fig. 22. Approximation of the experimental data for case 9, using the *k* exponential formulation.

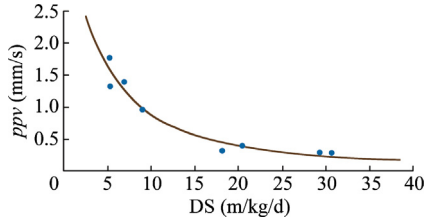

Fig. 23. Approximation of the experimental data for case 10, using the k exponential formulation.

As noted in Fig. 22, the values of the parameters referred to Eq. (12) are: *A* is 49,67, *b* 0,0232, *K* 0,3333, and $d \sim 0$.

3.10. Case 10: open-pit limestone quarry

The experimental data come from a measurement campaign in a limestone quarry near Cuneo, Northern Italy. The curve, corresponding to Eq. (12), that best approximates the experimental points, is given in Fig. 23.

As noted in Fig. 23, the values of the parameters referred to Eq. (12) are: *A* is 3,6849, *b* 0,1707, *K* 0,7536, and *d* 1,1902.

3.11. Case 11: open-pit limestone quarry

The experimental data come from a campaign in a limestone quarry near Lucca, Central Italy. Drilling is performed with

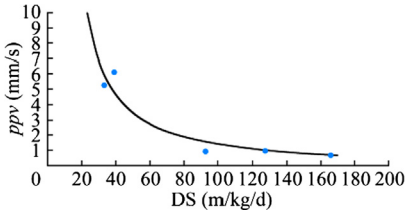

Fig. 24. Approximation of the experimental data for case 11, using the *k* exponential formulation.

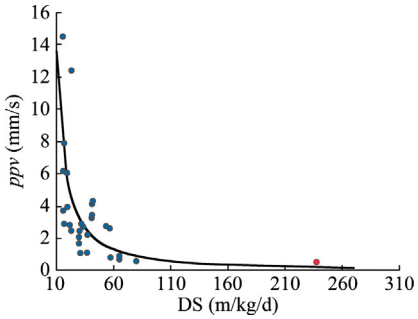

Fig. 25. Approximation of the experimental data for case 12, using the *k* exponential formulation.

76 mm vertical holes (length about 10 m). Stemming is 2 m, and blasting pattern is 2.5 m × 2.5 m. Bottom charge: slurry; column charge: ANFO. A blast is made by 400 kg of explosive, with a rock production of about 3000–4000 t, and a powder factor of 0.25–0.3 kg/m^3. Initiation is by long delay (500 ms) nonel detonators in the blast-holes, short delay (25 ms units) at the surface.

The curve, corresponding to Eq. (12), that best approximates the experimental points, is given in Fig. 24.

As noted in Fig. 24, the values of the parameters referred to Eq. (12) are: *A* is 313,02, *b* 0,0238, *K* 0,2584, *d* 0.

3.12. Case 12: civil tunnel in gneiss and mica-schists

The data come from a campaign of blast tests near to the future entrance of a 120 m^2 cross-section civil tunnel. It had to be excavated close to a small mountain village mainly consisting of stone buildings, some of them of historical importance. The campaign of experimental measurements was required for evaluating the behavior of the rock against vibrations, in order to preserve the integrity of such buildings. The rock mass consists of a succession of minute gneiss and mica-schists. On the surface, there is sometimes a modest debris cover. The following characteristics of the rock mass were known: GSI = 48; cohesion c = 0.85 MPa; friction angle $\phi = 50°$; elastic modulus E = 8250 MPa; Q = 2.44.

The curve, corresponding to Eq. (12), that best approximates the experimental points, is given in Fig. 25.

As noted in Fig. 25, the values of the parameters referred to Eq. (12) are: *A* is 48477, *b* 35,998, *K* 0,7735, and *d* 0,0094. Blue dots: measures recorded during blast tests; red dot: measure recorded during a production blast.

It is appreciable that the only measure recorded during the production blast (red dot), with a *ppv* of 0.55 mm/s (all others registrations were lower, since they have not reached the trigger threshold of the instrument of 0.5 mm/s) is well approximated by the curve obtained from the blast test (blue dots), even though they are characterized by much lower scaled distances.

4. Discussion

Data from the 12 case studies were analysed using four commonly employed site laws:

$$\text{Duvall \& Petkof} - \text{USBM}\ (1959): ppv = K \cdot \left(\frac{R}{\sqrt{Q_{max}}}\right)^{-n} \tag{13}$$

$$\text{Ambraseys} - \text{Hendron}(1968): ppv = K \cdot \left(\frac{R}{Q_{max}^{1/3}}\right)^{-n} \tag{14}$$

$$\text{Langefors} - \text{Kihlström}(1973): ppv = K \cdot \left(\sqrt{\frac{Q_{max}}{R^{3/2}}}\right)^{n} \tag{15}$$

$$\text{Indian Standard Institution}(1973): ppv = K \cdot \left(\frac{Q_{max}}{R^{2/3}}\right)^{n} \tag{16}$$

For each of these laws, the constants *K* and *n* were calculated, with the site constants made explicit and, separately, the related errors listed. To compare the *expK* formulation with the four abovementioned site laws, for each site and for each case the following data were analysed: the error, the standard deviation of the *ppv* experimental values compared to those approximated by the correlation, a number from 1 to 5 representing a classification of relative law performance and the percentage difference between the formula producing the lowest error with respect to the others. The performance of the various laws was also verified for cases in which blast tests were not available by using a correlation obtained for a similar site (rock mass characteristics and operation type). Finally, it was determined to what extent *expK*, unlike other correlations examined, better approximates experimental points for both high and low values of scaled distance.

The results obtained, referred to the 12 experimental cases considered, are shown in Tables 1–12, where the meaning of the used symbols is: *K* and *n*: site constants obtained by the 4 site laws employed, listed as Tables 1–4. A: Correlation analyzed; B: error; C: standard deviation; D: performance classification; E: percentage difference compared to the best site law.

The performance of the five cases where blast tests were not available before the excavation (a correlation previously obtained for similar sites must be therefore applied) have been verified: seven measurements in limestone rock being available, the correlation obtained in one of these cases was applied to the others. By using, for example, the correlations obtained for case 4 to the other sites with the same rock type (cases 3, 5, 7, 9, 10, 11), the results of Table 13 were obtained.

By applying the correlations obtained for case 5 to the other sites (cases 3, 4, 7, 9, 10, 11), in limestone rocks (same rock type), the results of Table 14 were obtained.

By applying, in a further example, the correlations obtained for case 10 to the other sites (cases 3, 4, 5, 7, 9, 11) in limestone rocks, the results of Table 15 were obtained.

Tables 13–15 show that the Langefors-Kihlström and USBM correlations are more reliable when the blast tests are not available; in other cases, *K*-exponential formulation shows in 11 cases out of 12 a better performance: this is due both to the characteristics of the deformed exponential and to the higher number of parameters involved. From the analyses carried out, it seems that the expK is accurate but not very versatile; a further defect is that, if the blast tests are made with very similar charges or always with the same charge, the parameter *d*, which is the exponent of the charge per delay *Q*, in the former case tends to 0 and in the second is 0: this implies that blast tests must be made with different charges per delay, otherwise the correlation obtained would be independent

Table 1
Case 1: excavation of a trench.

A	*K*	*n*	B	C	D	E
ExpK			0,91	0,32	1	
[1]	380,75	1,254	4,82	0,73	3	+425
[2]	444,78	1,219	4,55	0,71	2	+395
[3]	206,044	1,6842	18,44	1,43	4	+1909
[4]	13,538	1,3225	146,15	4,03	5	+15829

Table 2
Case 2: marlstone mine.

A	*K*	*n*	B	C	D	E
ExpK			8228	15,79	4	+22,6
[1]	961,09	1,72	6728	14,28	2	+0,46
[2]	1,528	1,64	6697	14,25	1	
[3]	478,08	2,304	7119	14,69	3	+6,3
[4]	10,989	1,8235	8652	16,19	5	+29,19

Table 3
Case 3: limestone quarry.

A	*K*	*n*	B	C	D	E
ExpK			1566	9,32	1	
[1]	777,35	1,563	3158	13,71	4	+103
[2]	1108,9	1,604	3858	14,64	5	+146
[3]	520,06	2,0032	2713	12,28	3	+73
[4]	68,848	1,679	2422	11,6	2	+56

Table 4
Case 4: limestone quarry.

A	*K*	*n*	B	C	D	E
ExpK			2,13	0,65	1	
[1]	186,35	1,502	6,71	1,16	3	+214
[2]	344,06	1,479	16,72	1,83	5	+685
[3]	89,841	1,9808	4,62	0,96	2	+116
[4]	2,7174	1,5763	4,93	0,99	4	+131

Table 5
Case 5: shaft-tunnel system in limestone.

A	*K*	*n*	B	C	D	E
ExpK			4,79	0,56	1	
[1]	611,28	1,641	1066	8,43	2	+22174
[2]	863,09	1,725	1088	8,51	3	+22630
[3]	402,79	2,0486	1189	8,9	4	+24736
[4]	50,537	1,5052	2520	12,96	5	+52548

Table 6
Case 6: underground gypsum quarry.

A	*K*	*n*	B	C	D	E
ExpK			418	3,41	1	
[1]	474,36	1,489	431	3,46	3	+3,28
[2]	933,02	1,497	435	3,48	4	+4,16
[3]	241,15	1,9718	29	3,46	2	+2,86
[4]	9,0658	2,1034	453	3,55	5	+8,44

on the charge; however, this is not a problem if, for instance, the same charge per delay should always be employed and only the ppv-distance relationship has to be known.

The expK formulation approximates well the experimental points for both low and high values of the scaled distance. The graphs below present some example of this trend respect to the other examined prediction equations.

Fig. 26 shows how the *K*-exponential predictor formula approximates the experimental data of Case 3 better than the others for high scaled distance values. Fig. 27 shows how the *K*-exponential predictor formula approximates the experimental points of Case 5 better than the others for both low and high scaled distance values. Fig. 28 shows how the *K*-exponential predictor formula approximates the experimental points of Case

Table 7
Case 7: limestone quarry.

A	*K*	*n*	B	C	D	E
ExpK			64,19	0,84	1	
[1]	701,43	1,465	65,52	0,853	4	+2,07
[2]	1137,3	1,465	65,52	0,853	5	+2,08
[3]	432.62	1,9529	65,47	0,852	2	+1,99
[4]	38,612	2,1971	65,48	0,852	3	+2,01

Table 8
Case 8: marlstone mine.

A	*K*	*n*	B	C	D	E
ExpK			167	2,19	1	
[1]	744,27	1,547	359	3,2	3	+114
[2]	1808,8	1,593	353	3,18	2	+111
[3]	285,8	1,9573	403	3,34	4	+141
[4]	5,8706	1,3617	815	4,83	5	+387

Table 9
Case 9: limestone quarry.

A	*K*	*n*	B	C	D	E
ExpK			529	3,89	1	
[1]	746,05	1,411	764	4,67	3	+44,5
[2]	1188,8	1,411	760	4,66	2	+43,7
[3]	468,04	1,8814	768	4,68	4	+45,3
[4]	45,379	2,1156	789	4,75	5	+49,3

Table 10
Case 10: limestone quarry.

A	*K*	*n*	B	C	D	E
ExpK			0,14	0,13	1	
[1]	3033,7	1,842	0,27	0,18	4	+99
[2]	16,307	1,993	0,61	0,28	5	+339
[3]	449,75	2,131	0,18	0,15	3	+28
[4]	2,4519	1,2322	0,17	0,14	2	+19

Table 11
Case 11: limestone quarry.

A	*K*	*n*	B	C	D	E
ExpK			2,69	0,73	1	
[1]	298,4	1,397	2,8231	0,75	4	+4,63
[2]	412,06	1,397	2,8239	0,75	5	+4,64
[3]	216,08	1,8625	2,8216	0,75	2	+4,58
[4]	43,03	2,0954	2,8221	0,75	3	+4,59

Table 12
Case 12: road tunnel in gneiss and mica-schists.

A	*K*	*n*	B	C	D	E
ExpK			173	2,49	1	
[1]	626,26	1,205	196	2,66	3	+13
[2]	820,68	1,374	175	2,51	2	+1,24
[3]	243,92	1,2299	226	2,89	4	+30
[4]	6,5733	0,1986	305	3,36	5	+74

9 better than the others for both low and high scaled distance values. Fig. 29 shows how the *K*-exponential predictor formula approximates the experimental points of Case 11 better than the others for both low and high scaled distance values.

The expK best approximates the experimental points both for low and for high values of scaled distances, unlike the other correlations, that tend to approximate well the experimental points only for a certain range of values of the scaled distances. This fact was also evidenced in the case 12, thanks to the good correspondence

Table 13
Position of the considered formulations in the approximation of data of different cases using the formulation obtained for case 4.

Formulation	Case 3	Case 5	Case 7	Case 9	Case 10	Case 11	Sum of position	Performances' classification
Expk	4	5	1	4	2	4	20	4
USBM	2	3	3	2	5	2	17	2
A-H	3	1	2	1	4	1	12	1
L-K	1	4	4	3	3	3	18	3
ISI	5	2	5	5	1	5	23	5

Table 14
Position of the considered formulations in the approximation of data of different cases using the formulation obtained for case 5.

Formulation	Case 3	Case 4	Case 7	Case 9	Case 10	Case 11	Sum of position	Performances' classification
Expk	4	4	4	2	4	3	21	3
USBM	2	2	2	3	1	4	14	2
A-H	3	1	5	4	3	5	21	3
L-K	1	3	1	1	2	2	10	1
ISI	5	5	3	5	5	1	24	4

Table 15
Position of the considered formulations in the approximation of data of different cases using the formulation obtained for case 10.

Formulation	Case 3	Case 4	Case 5	Case 7	Case 9	Case 11	Sum of position	Performances' classification
Expk	3	1	3	3	4	2	16	2
USBM	4	4	2	1	3	4	18	3
A-H	5	5	5	5	2	5	27	5
L-K	1	3	1	2	1	1	9	1
ISI	2	2	4	4	5	3	20	4

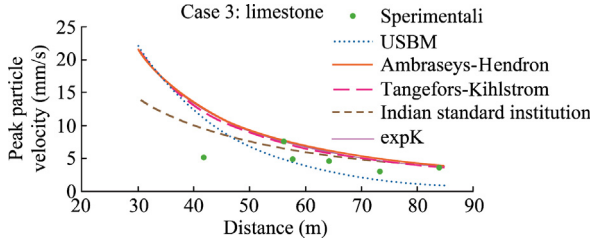

Fig. 26. How the K-exponential predictor formula approximates the experimental data of Case 3 better than the others for high scaled distance values.

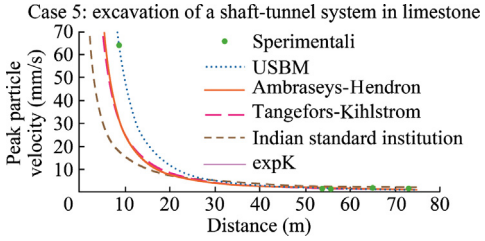

Fig. 27. How the K-exponential predictor formula approximates the experimental points of Case 5 better than the others for both low and high scaled distance values.

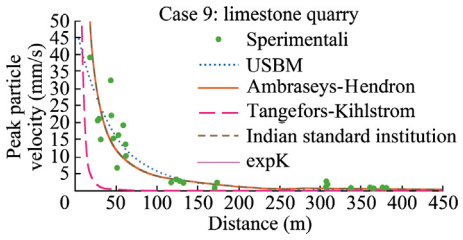

Fig. 28. How the K-exponential predictor formula approximates the experimental points of Case 9 better than the others for both low and high scaled distance values.

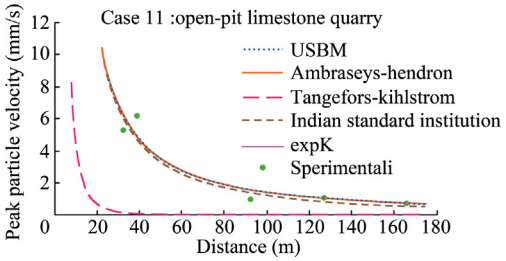

Fig. 29. How the K-exponential predictor formula approximates the experimental points of Case 11 better than the others for both low and high scaled distance values.

of the *ppv* recorded during a production blast with that predicted by the site law obtained on the basis of the measurements performed during the blast tests.

5. Conclusions

Data from 12 experimental case studies related to vibration measurement campaigns were analysed using both the most common site laws and the newly developed *K*-exponential formulation (expK). The new formulation was found to provide better results than the traditional laws in 11 out of 12 cases, producing a good approximation of experimental points. However, in the absence of blast tests, the classical laws used in the estimation of *ppv* values were more reliable. Since the charge per delay has an unknown exponent in the proposed formulation, blast tests must be carried out using different charges per delay; otherwise, an exponent equal to zero is obtained, producing a correlation independent on the charge per delay that is generally not useful in practice.

Nevertheless, the proposed formulation provides the advantage of offering a better correlation for experimental points than the other analysed site laws, both for low and high values of the scaled distance; this is in part attributable to the presence of a greater

number of parameters and in part to the nature of the deformed exponential contained in the function.

Interestingly, the *K*-formulation was able to reliably predict *ppv* values for high scaled distances (typical of production blasts) even when the *ppv*-scaled distance curve was drawn based on experimental points at low scaled distances (typical of blast tests). However, further tests are required to cover a larger number of cases, both blast tests and production blasts, in order to confirm the validity of the approach here presented.

References

[1] Ataei M, Sereshki F. Improved prediction of blast-induced vibrations in limestone mines using Genetic Algorithm. J Mining Environ 2017;82:291–304.
[2] Spathis AT, Wheatley M. Vibration modeling of three eDev^{TM} tunnel rounds in the Citybanan tunnel in Stockholm, rock fragmentation by blasting ISBN 978-0-415-62143-4. London: Taylor and Frencis Group; 2013. p. 771–91.
[3] Murthy VMSR, Dey K. Predicting overbreak from blast vibration monitoring in lake tap tunnel – a success story. Fragblast 2003;7(3):149–66.
[4] Oriard LL. Blasting effects and their control. SME Handbook, Littleton, Colorado; 1982, p. 1590–1603.
[5] Indian Standards Institute. Criteria for safety and design of structures subjected to underground blast. ISI, Bulletin IS-6922; 1973.
[6] Oriard LL. Observations on the performance of concrete at high stress levels from blasting. In: Proc. 6th Conf. on explosives and blasting technique, Tampa, Florida, USA. p. 1–10.
[7] Ghosh A, Daemen JK. A simple new blast vibration predictor (based on wave propagation laws). In: 24th US Symp. Rock Mechanics. p. 151–61.
[8] Page CH. Controlled blasting for underground mining. In: Proc. 13th Conf. on Explosives and Blasting Technique, Miami, Florida, USA. p. 33–48.
[9] Abersten L. Danni sul calcestruzzo dovuti a vibrazioni causate da brillamento di volate di mine. Explos Blast 1994;1:65–74.
[10] Singh SP, Lamond RD. Effect of decoupling and simultaneous detonation on blast vibrations. In: Proc. 11th Symp. on Explosives and Blasting Technique, Nashville, USA. p. 175–87.
[11] Singh PK, Vogt W. Ground vibration: prediction for safe and efficient blasting. Erzmetall 1998;51(10):677–84.
[12] Wild HW, Geuer M. Sprengarbeit beim Herstellen zweier Stollen und eines Schachtes im Schloss Neuschwanstein. Nobel Hefte 1999;2/3(65):89–98.
[13] Kahriman A. Analysis of ground vibrations caused by bench blasting at can open-pit lignite mine in Turkey. Environ Geol 2001;41:653–61.
[14] Singh PK, Roy MP. Damage to surface structures due to underground coal mine blasting: apprehension or real cause? Environ Geol. 2008;53:1201–11.
[15] Ambraseys NR, Hendron AJ. Dynamic behavior of rock masses. Rock Mechanics in Engineering, Stagg KG, Zeinkiewicz OC editor; 1968, p. 203-207.
[16] Duvall WI, Petkof B. Spherical propagation of explosion generated strain pulses in rock. US Bureau of Mines, R.I. 5483; 1959, p. 21.
[17] Langefors U, Kihlström B. The modern technique of rock blasting. New York: Wiley; 1973.
[18] Wiss J. Construction vibrations: state-of-the-art. J Geotech Eng Division 1981;107(2):167–81.
[19] Hagimori K, Furukawa K, Nakagawa K, Yokozeki Y. Study of non-blasting tunnelling by slot drilling method. In: Proc. 4th Int. Congr. Internatinal Journal of Rock Mechanics and Mining Sciences. p. A207–68. 325-478.
[20] Dowding C. Construction vibrations (Prentice Hall international series in civil engineering and engineering mechanics), ISBN: 9780964431317, xviii. Upper Saddle River, NJ: Prentice Hall Pub.; 1996. p. 610.
[21] Reynolds JM. An introduction to applied and environmental geophysics. Chichester: Wiley; 1997.
[22] Kim DS, Lee JS. Propagation and attenuation characteristics of various ground vibrations. Soil Dyn Earthquake Eng 2000;19(2):115–26.
[23] Mancini R, Cardu M, Sambuelli L. Vibrazioni indotte dallo scavo delle gallerie: sorgenti, misure, previsioni, rimedi, norme. Proc. MIR 2002, IX Ciclo di conferenze di meccanica e ingegneria delle rocce "Le opere in sotterraneo e il rapporto con l'ambiente". Patron Ed., Torino; 2002, p. 293–328.
[24] Blair D. Seismic radiation from an explosive column. Geophysics 2010;75(1):E55–65.
[25] Yan WM, Tham LG, Yuen KV. Reliability of empirical relation on the attenuation of blast-induced vibrations. Int J Rock Mech Min Sci 2013;59:160–5.
[26] Ahn JK, Park D. Prediction of near-field wave attenuation due to a spherical blast source. Rock Mech Rock Eng 2017:1–15.
[27] Kaniadakis G. Non-linear kinetics underlying generalized statistics. Phys A 2001;296:405–25.
[28] Abe S. A note on the q-deformation-theoretic aspect of the generalized entropies in nonextensive physics. Phys Lett A 1997;224:326–30.
[29] Acharya R, Narayana Swamy P. J Phys A: Math Gen 1994;27:7247.
[30] Anteneodo C, Plastin AR. J Phys A: Math Gen 1999;32:1089.
[31] Biedenharn LC. The quantum group SUq (2) and a q-analogue of the boson operators. J. Phys. A 1989;22:L873.
[32] Borges EP, Roditi I. A family of nonextensive entropies. Phys. Lett. A 1998;246:399.
[33] Buyukkilic F, Demirhan D. A fractal approach to entropy and distribution functions. Phys. Lett. A 1993;181:24.
[34] Frank TD, Daffertshofer A. Nonlinear Fokker-Planck equations whose stationary solutions make entropy-like functionals stationary. Phys A 1999;272:497.
[35] Greenberg OW, Mohapatra RN. Phenomenology of small violations of Fermi and Bose statistics. Phys. Rev. D 1989;39:2032.
[36] Landsberg PT, Vedral V. Distributions and channel capacities in generalized statistical mechanics. Phys. Lett. A 1998;247:211.
[37] Papa ARR. On one-parameter-dependent generalizations of Boltzmann-Gibbs statistical mechanics. J Phys A: Math Gen 1998;31:5271.
[38] Sharma BD, Mittal DP. New nonadditive measures of entropy for discrete probability distributions. J Math Sci 1975;10:28–40.
[39] Tsallis C. Possible generalization of Boltzmann-Gibbs statistics. J Stat Phys 1988;52:479.
[40] Imparato D, Trivellato B. Extended exponential models. In: Gibilisco P, Riccomagno E, Rogantin MP, Wynn HP, editors. Algebraic and Geometric Methods in Statistics. Cambridge University Press; 2010. p. 307–26.
[41] Kaniadakis G, Lavagno A, Quarati P. Kinetic approach to fractional exclusion statistics. Nucl Phys B 1996;466:527.
[42] Kaniadakis G, Lavagno A, Quarati P. Kinetic model for q-deformed bosons and fermions. Phys Lett A 1997;227:227.
[43] Kaniadakis G, Lapenta G. Microscopic dynamics underlying anomalous diffusion. Phys Rev E 2000;62:3246.
[44] Biermann PL, Sigl G. Lectures notes in physics. Berlin: Spring-Verlag; 2001.
[45] Wilk G, Wlodarczyk Z. Phys Rev D 1994;50:2318.
[46] Walton DB, Rafelski J. Phys Rev Lett 2000;84:31.
[47] Solomon TH, Weeks ER, Swinney HL. Phys Rev Lett 1993;71:3975.
[48] Antonia RA, Phan-Thien N, Satyoparakash BR. Phys Fluids 1981;24:554.
[49] Boghosian BM. Phys Rev E 1996;53:4754.
[50] Kasahara K. Earthquake mechanics. Cambridge: Cambridge University Press; 1981.
[51] Ausloos M, Ivanova K. Phys Rev E 2001;63:047201.
[52] Lu ET, Hamilton RJ. Astrophys J 1981;380:89.
[53] Niklas KJ, Amer J. Botany 1994;81:134.
[54] Nacher JC, Ochiai T. Phys Lett A 2008;372:6202.
[55] Plerou V, Gopikrishnan P, Nunes Amaral LA, Gabaix X, Stanley HE. Phys Rev E 2000;62:R3023.
[56] Gabaix X, Gopikrishnan P, Plerou V, Stanley HE. Nature 2003;423:267.
[57] Trivellato B. The minimal k-entropy martingale measure. Int J Theor Appl Finance 2012;15:1–22.
[58] Trivellato B. Deformed exponentials and applications to finance. Entropy 2013;15(9):3471–89.
[59] Moretto E, Pasquali S, Trivellato B. Option pricing under deformed Gaussian distributions. Phys A 2016;446:246–63.
[60] Blank A, Solomon S. Phys A 2000;287:279.
[61] Wichmann S, Stauer D, Lima FWS, et al. Trans Phil Soc 2007;105:126.
[62] Kosmidis K, Kalampokis A, Argyrakis P. Phys A 2006;366:495.
[63] Roberts DC, Turcotte DL. Fractals 1998;6:351.
[64] Clauset A, Young M, Gleditsch KS. J Conflict Resolut 2007;51:58.
[65] Kaniadakis G. H-theorem and generalized entropies within the framework of nonlinear kinetics. Phys Lett A 2001;288:283.
[66] Kaniadakis G. Statistical mechanics in the context of special relativity. Phys Rev E 2002;66:056125.
[67] Kaniadakis G. Statistical mechanics in the context of special relativity II. Phys Rev E 2005;72.
[68] Ak H et al. Evaluation of ground vibration effect of blasting operations in a magnesite mine. Soil Dyn Earthquake Eng 2009;29(4):669–76.
[69] Hao H, Wu C. Scaled-distance relationships for chamber blast accidents in underground storage of explosives. Fragblast 2001;5(1–2):57–90.
[70] Saadat M, Khandelwal M, Monjezi M. An ANN-based approach to predict blast-induced ground vibration of Gol-E-Gohar iron ore mine Iran. J Rock Mech Geotech Eng 2014;6(1):67–76.
[71] Giraudi A, Cardu M, Kecojevic V. An assessment of blasting vibrations – a case study on quarry operation in Italy. Am J Environ Sci 2009;5(4):467–73.
[72] Cardu M, Giaraudi A, Lovera E. An example of preliminary seismic survey to evaluate the feasibility of blasting works in proximity of a sensitive monument. 4th World conference on explosives and blasting techniques, 9-11 September, Wien, Austria, 2007.
[73] Cardu M, Dompieri M, Seccatore J. Complexity analysis of blast-induced vibrations in underground mining: a case study. Mining Science and Technology 2012;22:7. Elsevier Ed., 7pp.